

# Elucidation of Strong Cooperative Effects Caused by Dispersion Interactions in a Recognition-Mediated Diels–Alder Reaction

Arne Dieckmann\* and K. N. Houk\*

Department of Chemistry and Biochemistry, University of California, Los Angeles, 607 Charles E. Young Drive, Los Angeles, California 90095-1569, United States

## S Supporting Information

**ABSTRACT:** Cooperative effects caused by dispersion interactions between dienes and dienophiles in a so-called self-replicating system have been evaluated by density functional theory. A variety of functionals is tested for the elucidation of reactant complex stabilities. Dispersion interactions between dienes and dienophiles result in additional stabilizations of up to 10 kcal mol<sup>−1</sup>. These effects should be taken into account in future experimental studies and can be exploited to design more efficient systems.

## ■ INTRODUCTION

The reactants in Diels–Alder reactions can form complexes that are evident by the appearance of a charge-transfer band in UV spectra.<sup>1–5</sup> These attractive interactions are especially strong for polar dienes and dienophiles and mainly caused by dispersion. However, in most cases, free energies of complex formation are close to 0 kcal mol<sup>−1</sup> as the negative enthalpy resulting from dispersion interactions between the reactants is compensated by a negative entropic term associated with bringing two molecules together. Thus, the complexes do not have significant kinetic consequences in most cases. We suspected that complex formation will be more favorable in (pseudo)unimolecular Diels–Alder reactions. The diene and dienophile can still adopt an arrangement allowing attractive interactions, but the negative entropy of complex formation is significantly reduced, rendering the association more favorable in terms of free energy. This effect could impact the thermodynamics and kinetics of the reaction significantly, but might not be obvious from experimental data.

Here we report on accurate quantum-mechanical calculations using density functional theory (DFT) to identify complexation energetics in Diels–Alder reactions. The reaction we studied occurs in a so-called chemical self-replicating system,<sup>6,7</sup> which was analyzed experimentally by Philp and co-workers in 2005.<sup>8</sup> A simplified mechanistic model of this system is depicted in Figure 1. It is based on a Diels–Alder reaction between maleimide **A** and furan **B** yielding products *endo*- and *exo*-**C**. Both products can bind **A** and **B** by hydrogen-bonding between the amidopyridine-carboxyl recognition sites to form an [ABC] complex, thereby reducing the entropy of activation of the subsequent Diels–Alder reaction yielding product duplex [C<sub>2</sub>]. It has been shown experimentally that *endo*-**C** and *exo*-**C** both exclusively catalyze their own formation and do not engage in crosscatalysis due to mutual geometric incongruity.<sup>8</sup> A central assumption made in the analysis of this and similar systems<sup>9–19</sup> is that the stability of the catalytic species [ABC] is exclusively governed by hydrogen bonding. In other words, if one knew the free energy change for the association of a single amidopyridine-carboxyl recognition site, the free energy of complex formation for [ABC] would be twice as large. The

reason for this is that the equilibrium constant for the association of a single amidopyridine-carboxyl recognition site can be quantified experimentally in a model system, while the stability of [ABC] cannot be measured directly. As a consequence, interactions between the diene and dienophile are assumed to be of minor importance for the stability of [ABC].

The size of the system under investigation precludes the use of wave function methods like CCSD(T), which are able to correctly describe the nonlocal long-range correlation effects underlying dispersion interactions. CCSD(T) in the complete basis set limit is able to produce energies of chemical accuracy (<1 kcal mol<sup>−1</sup>) for noncovalent interactions,<sup>20</sup> and its reliable performance is unmatched by computationally less demanding methods. Hobza et al. have published a number of studies<sup>20,21</sup> as well as the S22<sup>22</sup> and S66<sup>23</sup> databases for a variety of small molecule complexes using this approach. However, for systems of 100 atoms or more, accurate wave function methods require considerable computational resources. In addition, thermal corrections as well as free energies of solvation are needed in order to reproduce experimentally determined equilibrium constants. Therefore, highly accurate electronic energies do not guarantee a good agreement with experiments unless the other terms can be obtained with similar accuracy.

DFT is much more economical than coupled cluster methods and offers a good compromise between accuracy and performance. Unfortunately, most exchange-correlation functionals do not account for long-range correlation, but empirical dispersion corrections such as D3 developed by Grimme can be added to DFT energies to correct for this failure. This correction has been shown to yield excellent results in comparison to CCSD(T) benchmark calculations.<sup>24,25</sup> Another approach is to include dispersion interactions in the parametrization of a functional. The so-called Minnesota functionals by Truhlar (e.g., M06-2X)<sup>26</sup> are examples of this strategy and show very good performance for midrange

**Special Issue:** Berny Schlegel Festschrift

**Received:** July 26, 2012

**Published:** September 12, 2012



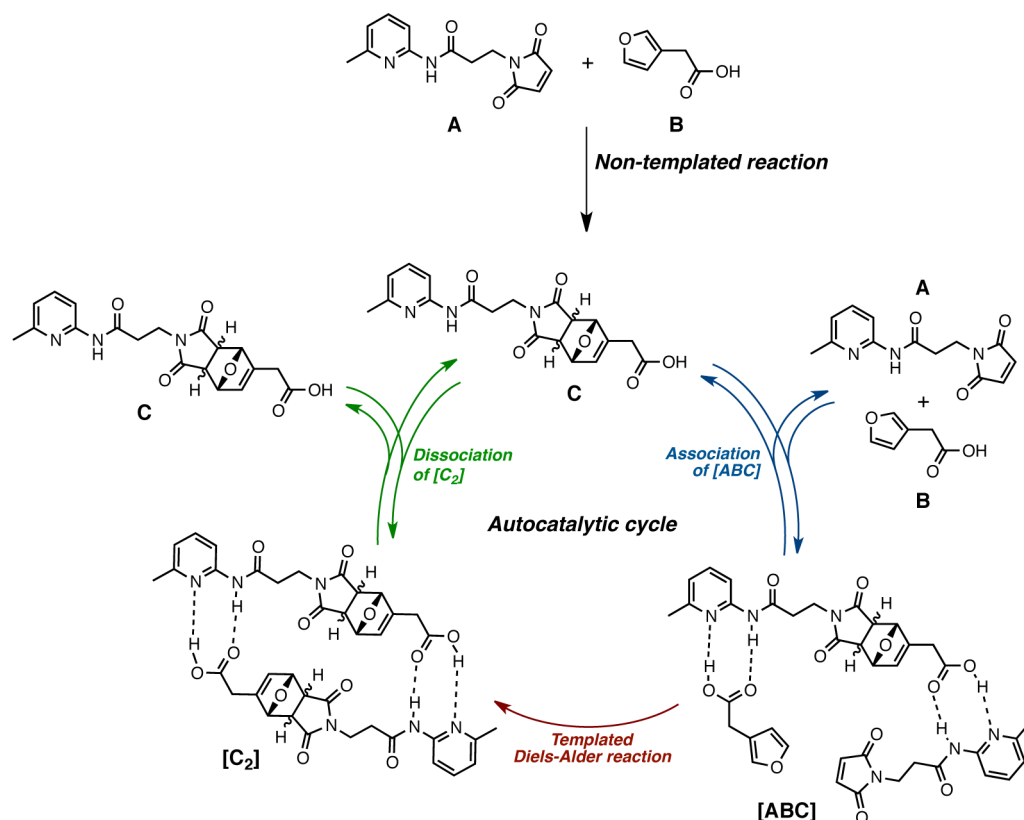


**Figure 1.** Minimal model of the self-replicating system discussed here. *endo* as well as *exo* products can be formed, and both exclusively catalyze their own formation.

dispersion effects in addition to their remarkable performance for thermodynamics and kinetics. We chose to take advantage of these functionals and to test them with empirical dispersion corrections to capture long-range dispersion effects. As our interest is in the quantification of cooperative effects in complex formations, the basis set superposition error needs to be minimized in order to avoid unphysical attractive interactions, which we did by employing large basis sets. A similar approach has recently been shown to yield accurate calculated stabilities for complexes based on dispersion interactions.<sup>27</sup>

In the following, we will first validate our computational procedure by comparing calculated stabilities of charge-transfer complexes to experiments. A number of different functionals are expected to be useful in this regard and have been evaluated. Afterward, we will demonstrate the existence of strong dispersion interactions in various complexes of the self-replicating system (Figure 1), making the assumption of additivity of complex energies to be inaccurate. Our results extend the experimental study by Philp and co-workers<sup>8</sup> and lead to a better understanding of this and similar systems.

## COMPUTATIONAL METHODS

Conformers were located with the mixed-torsional/low-mode Monte Carlo sampling algorithm as implemented in Maestro 9.3<sup>28</sup> using the OPLS-2005 force field<sup>29</sup> with a GB/SA solvation model for chloroform and an energy cutoff of 10 kcal mol<sup>-1</sup>. Structures with a heavy atom RMSD less than 2.0–3.0 Å were assumed to be the same conformer. The remaining structures (about 30) were optimized with the dispersion-corrected B97D density functional<sup>30</sup> and a 6-31G(d,p) basis set using loose convergence criteria. Subsequent geometry

optimizations of structures within 5.0 kcal mol<sup>-1</sup> of the global minimum employed B97D/6-31G(d,p) with tight convergence criteria. Solvation by chloroform was taken into account with the IEFPCM solvation model,<sup>31</sup> which was applied to both optimizations as well as frequency calculations. Thermal corrections were calculated from unscaled vibrational frequencies at the same level of theory for a standard state of 1 mol L<sup>-1</sup> and 298.15 K, although the experimental study employed a temperature of 308 K and lower concentrations. We found a good agreement with available experimental data using these conditions in benchmark calculations and believe other sources of errors to be more significant. Entropies were corrected for the breakdown of the harmonic oscillator approximation at low frequencies by raising all harmonic frequencies below 100 cm<sup>-1</sup> to 100 cm<sup>-1</sup>.<sup>32</sup> The resulting free energies refer to Gibbs energies. All stationary points were characterized and confirmed by vibrational analysis. Electronic energies were obtained from single points on the B97D/6-31G(d,p) geometries using the M06-2X meta-hybrid functional<sup>26</sup> and IEFPCM<sup>31</sup> with a def2-TZVPP<sup>33</sup> basis set to reduce the basis set superposition error (BSSE).<sup>34</sup> Grimme's D3 dispersion correction<sup>24</sup> (zero-damping) was also added to the M06-2X energies to determine if the performance was improved for these complexes.<sup>35</sup> All calculations were performed with Gaussian 09.<sup>36</sup>

## RESULTS AND DISCUSSION

**Quantifying Dispersion Interactions and Hydrogen Bonding.** *Dispersion Interactions in Model Systems.* We began by testing our computational procedures on the basis of experimentally characterized charge-transfer complexes. The experimental stabilities of reactive complexes (such as Diels–

Alder reactants) are not as reliable as those of unreactive ones, and most of the benchmark data are of the latter variety. The exception is complex 5 between 9,10-dimethylantracene and tetracyanoethylene (Figure 2), a combination that is reactive

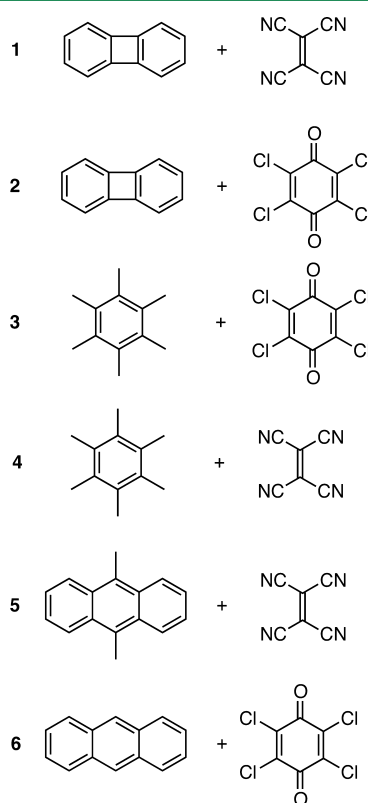


**Figure 2.** Experimentally characterized charge-transfer complexes used for testing our computational procedures.<sup>3,37–39</sup>

but also forms a stable complex. Six bimolecular charge-transfer complexes were chosen from the literature (Figure 2),<sup>3,37–39</sup> and the complex stabilities were calculated using different methods (Table 1). We used the well-tested B97D functional<sup>30</sup> for optimizations and thermal corrections as it is cheap in terms

of computational time and can be applied conveniently to larger complexes.

Optimized geometries of all complexes are depicted in Figure 3. In general, complexes 3 and 4 involving hexamethylbenzene feature larger interplanar distances of 3.16 Å between the constituents than 1, 2, and 5 (~3.0 Å). This is due to steric repulsion caused by the methyl groups. Complex 6 displays the largest interplanar distance (3.19 Å). A comparison of the calculated geometry of complex 4 with that of its crystal structure (obtained from a 2:1 hexamethylbenzene-tetracyanoethylene crystal)<sup>42</sup> reveals a good agreement with the experimental interplanar distance of 3.17–3.19 Å. Chloranil complex 6 shows a similar interplanar distance as a recently published crystal structure of an *o*-chloranil-styrene complex (~3.20 Å).<sup>43</sup> In general, all interplanar distances are shorter than the typical 3.4–3.5 Å in other arene–arene complexes.<sup>22,23</sup>

Experimental free energies of complex formation vary between +0.5 kcal mol<sup>−1</sup> for complex 1 and −3 kcal mol<sup>−1</sup> for complex 5 (entry 11 in Table 1). These are reproduced by M06-2X-D3 employing a def2-TZVPP basis set and IEFPCM to model solvation with a mean absolute deviation (MAD) of 1.2 kcal mol<sup>−1</sup> (entry 8 in Table 1). In particular, relative stabilities are in qualitative agreement with experimental numbers except for complexes 3 and 6, whose experimental free energies are essentially identical. Independent experimental measurements of free energies of complex formation can vary by as much as 0.9 kcal mol<sup>−1</sup>; rendering this agreement is very reasonable. Calculations using the same method without additional empirical dispersion corrections (entry 9 in Table 1) show that M06-2X energies benefit from D3 corrections, as free energies without D3 corrections are 0.8–1.7 kcal mol<sup>−1</sup> more positive and deviate more from experimental values. This effect is expected to be even more pronounced in larger systems, as the D3 corrections mainly add missing long-range dispersion effects to M06-2X. Implicit solvation by IEFPCM for dichloromethane raises complex formation energies by 1.5–2.9 kcal mol<sup>−1</sup> in comparison to gas-phase values (entry 7). Gas phase stabilities of complexes 1, 2, and 6 are closer to experimental results than those calculated with IEFPCM, but complex stabilities for 3, 4, and 5 are substantially overestimated by 2.2–3.1 kcal mol<sup>−1</sup>. Thus, the use of an implicit solvation model leads to more consistent results. In order to

**Table 1.** Calculated Free Energies of Complex Formation (in kcal mol<sup>−1</sup>) for the Charge-Transfer Complexes Given in Figure 4 Using Different Methods<sup>a</sup>

entry	geometry, ZPE, and thermal corrections	electronic energy	complex					
			1	2	3	4	5	6
1	B3LYP/6-31G(d,p) (gas phase)	B3LYP/6-31G(d,p) (gas phase)	+7.6	+10.3	+9.3	+5.6	+6.3	+11.4
2		B3LYP/6-31G(d,p)	+9.4	+11.2	+11.0	+8.0	+7.5	+12.4
3		B3LYP/def2-TZVPP	+11.9	+13.7	+13.0	+10.9	+9.9	+13.4
4	B97D/6-31G(d,p)	B97D/6-31G(d,p)	−2.8	−3.5	−3.1	−5.6	−10.4	+0.9
5		MPWB1K-D3/def2-TZVPP	+0.9	−0.1	−1.7	−0.2	−5.7	+0.4
6		MPW1B95-D3/def2-TZVPP	+0.7	−0.2	−1.5	−1.9	−6.0	+0.8
7		M06-2X-D3/def2-TZVPP (gas phase)	+0.4	+0.4	−2.3	−3.8	−5.2	±0.0
8		M06-2X-D3/def2-TZVPP	+2.2	+1.5	−0.2	−0.9	−3.4	+1.5
9		M06-2X/def2-TZVPP	+3.0	+2.6	+1.5	+0.3	−2.3	+2.9
10		M06-2X-D3/def2-QZVP	+2.3	+2.1	+0.4	−0.8	−3.3	+2.1
11	experimental free energies:		+0.5	+0.3	+0.1	−0.7	−3.0	−0.1

<sup>a</sup>IEFPCM has been used to model solvation by dichloromethane.

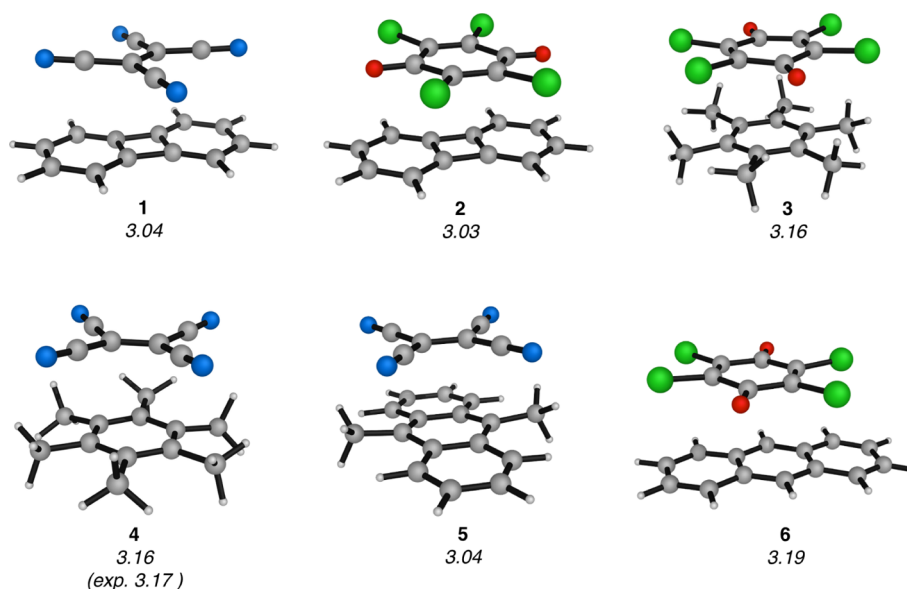


**Figure 3.** Optimized geometries of charge-transfer complexes (B97D/6-31G(d,p)). Interplanar distances for each complex are given in Å. The experimental interplanar distance for complex 4 refers to its crystal structure.<sup>37,40,41</sup>

probe the convergence and BSSE of the TZVPP basis set, we also employed the much larger QZVP basis (entry 10).<sup>33</sup> For all complexes except the ones with chloranil, free energies of complex formation become more positive by 0.1 kcal mol<sup>-1</sup>. Chloranil complexes display a change of 0.6 kcal mol<sup>-1</sup>. These results correspond to a BSSE of less than 5% of the electronic interaction energy in the TZVPP basis. As this basis is much more economical in terms of computational time than the QZVP basis (factor of 7), we used it throughout this study to obtain reliable electronic energies.

In addition to the M06-2X functional, we also calculated free energies of complex formation with the MPWB1K (entry 5) and MPWB95 (entry 6) functionals, as these have been shown to display a very good performance for thermodynamics and kinetics.<sup>44</sup> In fact, MADs from experiments are only 1.1 kcal mol<sup>-1</sup> for both of these, but they show the single largest deviation (2.7 and 3.0 kcal mol<sup>-1</sup>) for complex 5. As M06-2X performed equally well but is able to provide accurate results for both thermodynamics and kinetics, we used it for the calculation of larger systems studied here. To assess the importance of incorporating dispersion in our computational procedure, we calculated free energies of complex formation using the popular B3LYP functional<sup>45,46</sup> without any empirical dispersion corrections (entry 3). Not surprisingly, it yields dramatically different results. Free energies of complex formation exceed +10 kcal mol<sup>-1</sup> and do not predict any complex to be stable. While B3LYP has been shown to perform better with smaller basis sets in general,<sup>47–49</sup> our calculations show an improvement of only 1–3 kcal mol<sup>-1</sup>, probably caused by the BSSE (entry 2). Following the trend observed for M06-2X, gas phase values predict more stable complexes (entry 1). The method used for optimizations (B97D/6-31G(d,p)) shows an unsatisfactory performance with respect to electronic energies (entry 4). While it provides good geometries, all energies of complex formation are strongly overestimated (in part due to the BSSE) and thus separate single point calculations using a more reliable functional and larger basis set are necessary.

Next, we calculated the interaction enthalpy and free energy between a furan and maleimide moiety without recognition sites in chloroform to estimate the magnitude of stabilization that might occur in [ABC] complexes due to interactions between the diene and dienophile (Figure 4). Our dispersion

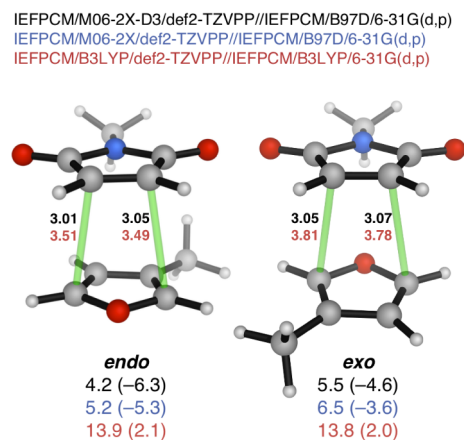


**Figure 4.** Calculated interaction free energies and enthalpies in parentheses in kcal mol<sup>-1</sup> for a complex between a model furan and maleimide. A properly dispersion-corrected method is compared with values obtained with the popular B3LYP functional. Distances are given in Å.

corrected approach, as described in Computational Methods, predicts negative enthalpies of -6.3 kcal mol<sup>-1</sup> for an *endo* and -4.6 kcal mol<sup>-1</sup> for *exo* arrangement, which are overcompensated by a negative entropic term, so that the free energy of complex formation is substantially positive. D3 corrections contribute a stabilization of 1 kcal mol<sup>-1</sup> in both cases. The *endo* conformation is more stable by 1.3 kcal mol<sup>-1</sup> than the *exo* conformation due to a larger overlap of the reactants, which is also reflected in slightly shorter distances between the carbon reaction centers. Either way, no stable complex is formed, and thus dispersive interactions should not impact bimolecular reactions. We also calculated complex



formation energies for the furan and maleimide using the B3LYP functional<sup>45,46</sup> (Figure 4). With relaxation of the geometries, the distance between the two rings increases to 3.5–3.8 Å and the enthalpic interaction is calculated to be repulsive. Further, enthalpies and free energies for *endo* and *exo* geometries are essentially identical. This demonstrates two things: First, important attractive interactions between dienes and dienophiles cannot be predicted by this approach. Second, these interactions are in fact based on dispersion and not on electrostatics.

**Hydrogen Bonding.** In order to quantify the amount of additional stabilization arising from dispersion interactions in hydrogen-bonded complexes, the contribution from hydrogen bonding alone has to be known. The association constant for a single carboxyl-amidopyridine interaction has been determined experimentally by NMR titration for a model system and corresponds to a free energy of complex formation of  $-3.4$  kcal mol<sup>-1</sup> (Figure 5).<sup>8</sup> We used the same model system to assess

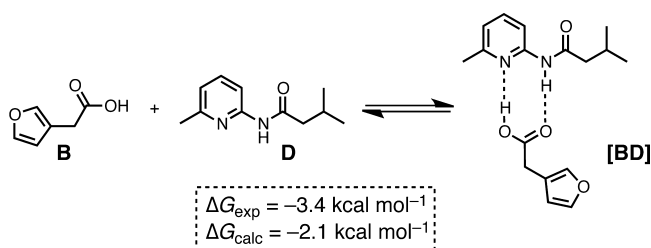


**Figure 5.** Experimental<sup>8</sup> and calculated free energy of complex formation for a model system.

hydrogen bonding, and our calculated value of  $-2.1$  kcal mol<sup>-1</sup> underestimates this complex stability but is in reasonable agreement. Relative free energies for the formation of other complexes are expected to be even more reliable than this absolute value. Thus, in the absence of cooperativity [ABC] should display a calculated stability of about  $-4.2$  kcal mol<sup>-1</sup>, as twice the number of recognition sites are involved in its formation. [C<sub>2</sub>] on the other hand should be more stable than this due to a stabilizing chelate effect, unless unfavorable steric or electronic interactions are present.

**Cooperative Effects in [ABC] and [C<sub>2</sub>].** It was established experimentally that each product *endo*-C and *exo*-C exclusively catalyzes its own formation.<sup>8</sup> In other words, only diastereomeric autocatalysis and no crosscatalysis is operative in the system. However, there are two enantiomers for each product, and each of these might engage in auto- or crosscatalysis. It proved impossible to distinguish between enantiomers experimentally,<sup>8</sup> and the kinetic analysis was based on the assumption of equal catalytic potency of all enantiomers. Thus, we will limit our theoretical study to a single enantiomer of each *endo*-C and *exo*-C in order to keep the number of complexes and conformations manageable. While subtle differences in stability might exist between the complexes participating in enantiomeric auto- and crosscatalytic cycles, the cooperative effects identified by our study will be present in all pathways. As it is not our goal to make accurate quantitative predictions about the efficiency of different catalytic cycles, but to demonstrate the existence of strong stabilizing interactions in supramolecular complexes, this simplification will not impact our results.

In order to construct [ABC] complexes, we employed the following procedure: First, we performed a conformational

search of [C<sub>2</sub>] complexes and identified low energy conformers by their B97D/6-31G(d,p)/IEFPCM energies after optimization at the same level. Afterward, a corresponding [ABC] complex was constructed for each [C<sub>2</sub>] complex by increasing the distance between the furan and maleimide unit to about 3 Å and reoptimizing. As a consequence, [ABC] complexes with an antiperiplanar alignment of the furan and maleimide ring were obtained, which we will term to be in a reactive conformation. A second conformational search was performed which started from [ABC] complexes and constrained the carboxyl-amidopyridine hydrogen bonds. This search was not explicitly biased toward reactive conformations and thus allowed us to check whether other random conformations were lower in energy. Final enthalpies and free energies were obtained as described in the Computational Methods. While free energies derived from vibrational frequencies for flexible molecules certainly include some error, the effects to be discussed are much larger than these errors. In addition, our conclusions are backed up by the corresponding enthalpies, which are expected to be accurate.

**AB and [ABC] Complexes.** As mentioned above, the central assumption made when analyzing small organic replicators is that the formation of [ABC] is not affected by cooperative effects. This pragmatic approach reduces the number of variables in kinetic models (and therefore covariances between variables), as the association constant  $K_{[ABC]}$  is set to  $K_{[ABC]} = K_{[AB]}^2 \approx K_{[BD]}^2$  (Figure 6). This seems to be well-justified in light of the impossibility to quantify the stability of [ABC] or [AB] directly. For our computational study, this implies that  $\Delta G_{[ABC]} = 2 \times \Delta G_{[AB]} \approx 2 \times \Delta G_{[BD]} = -4.2$  kcal mol<sup>-1</sup> (Figure 6). However, a comparison of free energies of complex formation of the unreactive [BD] and reactive AB complex reveals that [AB] benefits from a significant attractive interaction, which does not arise from hydrogen bonding (Figure 6) but from a  $\pi$ -H interaction between the furan and maleimide. As the maleimide moiety is not present in [BD], this complex is less stable than [AB]. In other words, the separately determined equilibrium constant for [BD] is too small and needs to be corrected for application in a kinetic model of the full system.

Cooperative effects are even more pronounced in [ABC] complexes. The three most stable *endo*-[ABC] and *exo*-[ABC] complexes are displayed in Figure 6. Complex formation free energies are not close to  $\Delta G_{[ABC]} \approx -4.2$  kcal mol<sup>-1</sup> but are significantly more negative (up to  $-14.7$  kcal mol<sup>-1</sup>). This is especially surprising as they are given relative to the most stable conformations of *endo*-C and *exo*-C, featuring one or two intramolecular hydrogen bonds (Figure 6). The two intramolecular hydrogen bonds in *endo*-C are responsible for *endo*-[ABC] complexes being much less stable in general than their *exo* counterparts. D3 corrections account for a stabilization of about 5 kcal mol<sup>-1</sup> in *endo*-[ABC] and 6 kcal mol<sup>-1</sup> in *exo*-[ABC].

*endo*-[ABC]-1 represents the lowest-energy *endo* conformer located in our study and adopts an antiperiplanar arrangement of the maleimide and furan, just like *endo*-[ABC]-2. Both complexes benefit from favorable interactions between the furan and maleimide in an *endo*-arrangement as well as the two aromatic pyridine rings, resulting in free energies of complex formation of  $-7.3$  kcal mol<sup>-1</sup> and  $-6.0$  kcal mol<sup>-1</sup>, respectively. *endo*-[ABC]-3 is an example of a conformation in which the furan and maleimide are separated. Assuming that hydrogen bonding accounts for  $-4.2$  kcal mol<sup>-1</sup>, there is an additional

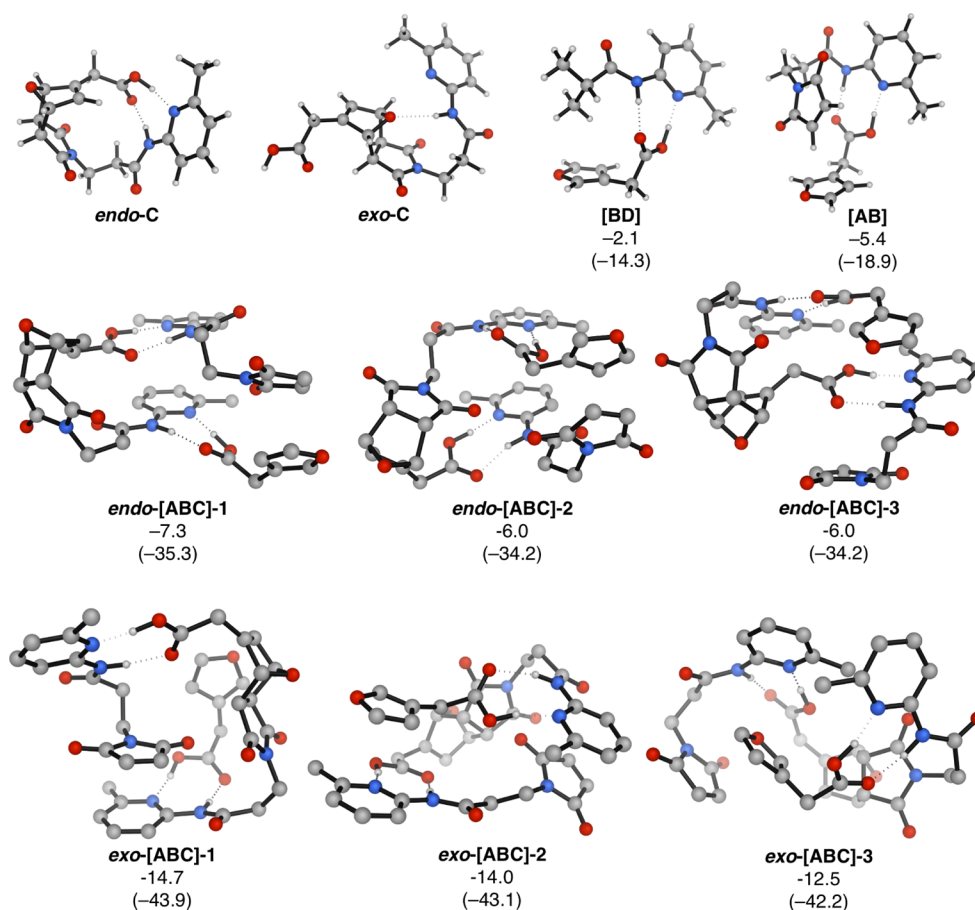


**Figure 6.** Structures and energies of some bimolecular and termolecular complexes. The three most stable *endo*-[ABC] and *exo*-[ABC] complexes are displayed (most hydrogen atoms are omitted for clarity). Free energies and enthalpies in parentheses are given in kcal mol<sup>-1</sup>.

stabilization of more than 3 kcal mol<sup>-1</sup> in terms of free energy. A comparison of the respective enthalpies reveals that all complexes are stabilized not only by dispersion but also by a complicated network of complementary electrostatic interactions between carbonyl oxygens and polarized hydrogen atoms.

Due to the presence of only one hydrogen bond in *exo*-C in contrast to two in *exo*-C, *endo*-[ABC] complexes are much more stable than *endo*-[ABC] complexes. They display remarkable free energies of complex formation of up to -14.7 and -14.0 kcal mol<sup>-1</sup> in *exo*-[ABC]-1 and *exo*-[ABC]-2, which translates into cooperative effects on the order of 10 kcal mol<sup>-1</sup>. Both of these do not resemble a reactive conformation but feature a large distance between the reaction centers. The electron-deficient maleimide engages in stacking interactions with the electron-rich pyridine ring, which is a better electron donor than the furan. In *exo*-[ABC]-3, the maleimide and furan are aligned in an antiperiplanar geometry, resulting in a smaller free energy of complex formation of -12.5 kcal mol<sup>-1</sup>. Nevertheless, the stability of all three complexes is extraordinary and has been underestimated by kinetic modeling based on experimental data.<sup>8</sup> To illustrate once more the necessity to take into account dispersion, we computed B3LYP/def2-TZVPP single point energies for these highly stabilized geometries. A comparison of enthalpies with our original calculations reveals a dramatic difference: While dispersion-corrected DFT predicts enthalpies on the order of -40 kcal mol<sup>-1</sup>, B3LYP enthalpies are between -1.9 and -4.4

kcal mol<sup>-1</sup>. Favorable dispersion interactions are interpreted as being repulsive, and thus these geometries could not have been located with B3LYP or any other functional lacking dispersion correction. Calculations with such functionals would lead to the wrong conclusion that the stability of [ABC] is exclusively dictated by hydrogen bonding. These findings agree well with those shown in Figure 4. Another important point is the size of the basis set used to assess the stability of these large complexes. We found that the smaller double- $\zeta$  basis used for optimization (6-31G(d,p)) overestimates complex stabilities by more than 10 kcal mol<sup>-1</sup>, presumably due to a large BSSE.

Our results demonstrate that the stability of [ABC] complexes cannot be approximated by adding up hydrogen bonds. In fact, the errors arising from applying this assumption to kinetic models are enormous and will lead to inaccurate values for fitted rate and equilibrium constants. Of course, our calculated free energies suffer from the inherent flexibility of the complexes, but these errors are still small compared to the magnitude of cooperativity. In addition, accurately calculated enthalpies support our findings. Another interesting aspect of our results is that reactive conformations can display a higher stability than those in which the reactive centers are far apart. A careful design process might take advantage of this by restricting the conformational space in such a way that dispersion interactions between the reactants and the pyridine ring are impossible.

**[C<sub>2</sub>] Complexes.** The dissociation of the [C<sub>2</sub>] complexes resulting from the ligation of A and B inside an [ABC] complex

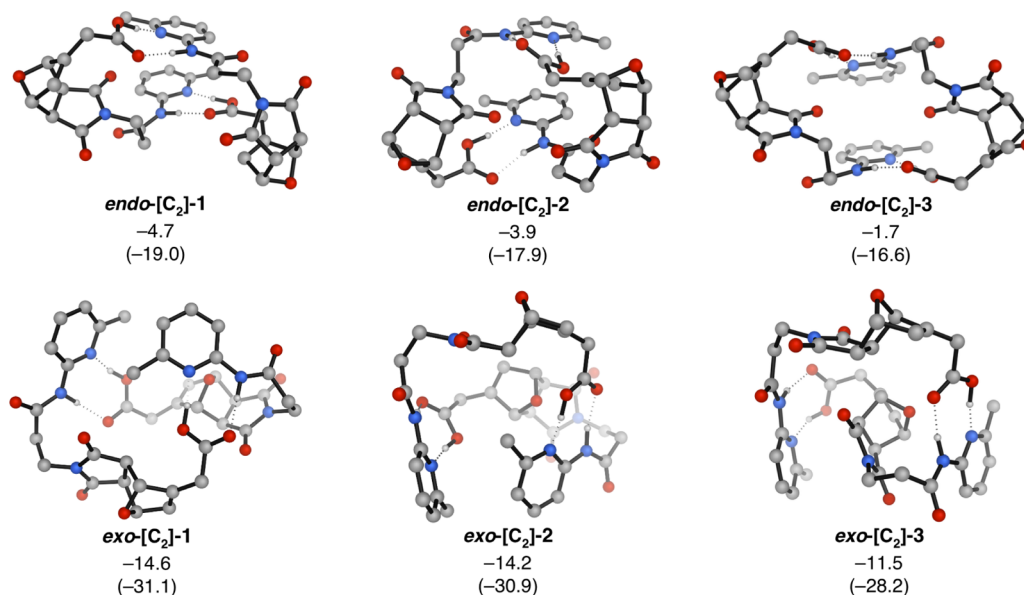


**Figure 7.** Geometries and complex formation free energies for the lowest energy  $[C_2]$  conformers. Most hydrogen atoms are omitted for clarity. Free energies and enthalpies in parentheses are given in  $\text{kcal mol}^{-1}$ .

closes the autocatalytic cycle (Figure 1). A sufficiently low stability of  $[C_2]$  is critical for good turnover, as a high stability with respect to  $[ABC]$  leads to product inhibition. However,  $[C_2]$  complexes are intrinsically stabilized by chelate cooperativity, which would have to be counterbalanced by less favorable enthalpic interactions than in  $[ABC]$  complexes.

The three lowest energy *endo*- $[C_2]$  and *exo*- $[C_2]$  complexes are displayed in Figure 7. As discussed before, *endo* duplexes are less stable than *exo* duplexes due to the ability of *endo*-C to form intramolecular hydrogen bonds. D3 corrections lower free energies of complex formation by about  $3.5 \text{ kcal mol}^{-1}$  for *endo*- $[C_2]$  and  $4 \text{ kcal mol}^{-1}$  for *exo*- $[C_2]$ . A comparison of the enthalpies of complex formation for  $[C_2]$  (Figure 7) and  $[ABC]$  (Figure 6) reveals  $[C_2]$  complexes to be more than  $10 \text{ kcal mol}^{-1}$  less favorable. We attribute this difference to the missing dispersion interactions between the furan, maleimide, and pyridine ring as well as to the introduction of some strain by the more rigid structures. However,  $[C_2]$  duplexes are still of comparable stability in terms of free energy and do not suffer from negative cooperativity. On the basis of kinetic modeling and force field calculations, the authors of the experimental study came to the conclusion that *endo*- $[C_2]$  as well as *exo*- $[C_2]$  complexes display the same stability as  $[BD]$  complexes due to steric congestion in the center.<sup>8</sup> By contrast, we find no steric repulsion and instead show that cooperative effects have a substantial influence on the stabilities of complexes.

These findings highlight the importance of understanding the attractive interactions between the maleimide, furan, and pyridine ring in  $[ABC]$  complexes. After ligation, these dispersion interactions cannot be operative anymore, and thus  $[C_2]$  complexes lack one additional source of stabilization. The ability to selectively stabilize  $[ABC]$  with respect to  $[C_2]$  leads to a stronger autocatalytic growth of the template<sup>7</sup> and is one of the biggest challenges when constructing artificial replicators. However, interactions between the diene and dienophile as a source of stabilization of  $[ABC]$  have not been recognized as such for any self-replicating system based on a Diels–Alder or 1,3-dipolar cycloaddition so far, because it is not immediately evident from the kinetics of these reactions.

## CONCLUSIONS

The goal of this computational study was to identify and quantify cooperative effects based on dispersion in a self-replicating system employing a pseudo-unimolecular Diels–Alder reaction. We focused on aspects that would be of help to an experimentalist analyzing or designing these kind of systems. On the basis of calculations on model systems, we expected a selective stabilization of termolecular complexes  $[ABC]$  due to significant dispersion interactions between the diene and dienophile. In fact, these were identified by our study and led to an additional stabilization of up to  $10 \text{ kcal mol}^{-1}$ . Up to now, cooperative effects have been completely neglected in the kinetic analysis and design of small organic replicators. However, we show here that existing kinetic models need to be extended to take such an additional stabilization of complexes into account, which will probably change the conclusions drawn from them. How exactly cooperativity can be incorporated in kinetic models without increasing the number of unknown variables substantially is not clear at the moment and is a challenge for experimentalists. We believe our results to be quite general and dispersion interactions to impact other (pseudo)-unimolecular Diels–Alder reactions as well.

In terms of methodology, our results highlight the need to apply dispersion corrected density functional theory in conjunction with large basis sets to obtain reliable energetics.<sup>27</sup> In addition, a thorough exploration of the conformational space utilizing an energetic ranking based on DFT energies is mandatory, as force field energies show no correlation with DFT results. Unfortunately, this procedure is quite expensive in terms of computational resources, preventing its routine application for large systems. However, it will be instructive to obtain thorough computational data for a number of systems to guide the experimental design in the future.

## ASSOCIATED CONTENT

### Supporting Information

Cartesian coordinates, energies, and thermodynamic corrections for all reported structures. This information is available free of charge via the Internet at <http://pubs.acs.org>.



## ■ AUTHOR INFORMATION

## Corresponding Author

\*E-mail: adieckmann@ucla.edu, houk@chem.ucla.edu.

## Notes

The authors declare no competing financial interest.

## ■ ACKNOWLEDGMENTS

This work used the Extreme Science and Engineering Discovery Environment (XSEDE), which is supported by National Science Foundation grant number OCI-1053575 as well as the UCLA Academic Technology Services (ATS) Hoffman Beowulf cluster. We are grateful to the Alexander von Humboldt foundation (Feodor Lynen fellowship to A.D.) and the National Science Foundation for support of this research through grant CHE-1059084 to K.N.H.

## ■ REFERENCES

- (1) Andrews, L. J.; Keefer, R. M. *J. Am. Chem. Soc.* **1955**, *77*, 6284–6289.
- (2) Cooper, A. R.; Crowne, C. W. P.; Farrell, P. G. *Trans. Faraday Soc.* **1966**, *62*, 18–28.
- (3) Kiselev, V.; Miller, J. J. *Am. Chem. Soc.* **1975**, *97*, 4036–4039.
- (4) Sustmann, R.; Dern, M.; Kasten, R.; Sicking, W. *Chem. Ber.* **1987**, *120*, 1315–1322.
- (5) Sustmann, R.; Korth, H.; Nüchter, U.; Siangouri Feulner, J.; Sicking, W. *Chem. Ber.* **1991**, *124*, 2811–2817.
- (6) Vidonne, A.; Philp, D. *Eur. J. Org. Chem.* **2009**, 593–610.
- (7) von Kiedrowski, G. *Bioorg. Chem. Front.* **1993**, *3*, 113–146.
- (8) Kassianidis, E.; Pearson, R. J.; Philp, D. *Org. Lett.* **2005**, *7*, 3833–3836.
- (9) Sinclair, A. J.; del Amo, V.; Philp, D. *Org. Biomol. Chem.* **2009**, *7*, 3308–3318.
- (10) Kassianidis, E.; Philp, D. *Chem. Commun.* **2006**, 4072–4074.
- (11) Kassianidis, E.; Philp, D. *Angew. Chem., Int. Ed.* **2006**, *45*, 6344–6348.
- (12) Pearson, R. J.; Kassianidis, E.; Slawin, A. M. Z.; Philp, D. *Chem.—Eur. J.* **2006**, *12*, 6829–6840.
- (13) Sadownik, J. W.; Philp, D. *Angew. Chem., Int. Ed.* **2008**, *47*, 9965–9970.
- (14) Allen, V. C.; Robertson, C. C.; Turega, S. M.; Philp, D. *Org. Lett.* **2010**, *12*, 1920–1923.
- (15) Tjivikua, T.; Ballester, P.; Rebek, J. J. *Am. Chem. Soc.* **1990**, *112*, 1249–1250.
- (16) Nowick, J. S.; Feng, Q.; Tjivikua, T.; Ballester, P.; Rebek, J., Jr. *J. Am. Chem. Soc.* **1991**, *113*, 8831–8839.
- (17) Wang, B.; Sutherland, I. O. *Chem. Commun.* **1997**, *16*, 1495–1496.
- (18) Kindermann, M.; Stahl, I.; Reimold, M.; Pankau, W. M.; von Kiedrowski, G. *Angew. Chem., Int. Ed.* **2005**, *44*, 6750–6755.
- (19) Dieckmann, A.; Beniken, S.; Lorenz, C. D.; Doltsinis, N. L.; von Kiedrowski, G. *Chem.—Eur. J.* **2011**, *17*, 468–480.
- (20) Riley, K. E.; Pitoňák, M.; Jurecka, P.; Hobza, P. *Chem. Rev.* **2010**, *110*, 5023–5063.
- (21) Hobza, P. *Acc. Chem. Res.* **2012**, *45*, 663–672.
- (22) Jurecka, P.; Sponer, J.; Cerny, J.; Hobza, P. *Phys. Chem. Chem. Phys.* **2006**, *8*, 1985–1993.
- (23) Rezáč, J.; Riley, K. E.; Hobza, P. *J. Chem. Theory Comput.* **2011**, *7*, 2427–2438.
- (24) Grimme, S.; Antony, J.; Ehrlich, S.; Krieg, H. *J. Chem. Phys.* **2010**, *132*, 154104–1–19.
- (25) Ehrlich, S.; Moellmann, J.; Grimme, S. *Acc. Chem. Res.* **2012**, DOI: 10.1021-ar3000844.
- (26) Zhao, Y.; Truhlar, D. G. *Theor. Chem. Acc.* **2008**, *120*, 215–241.
- (27) Grimme, S. *Chem.—Eur. J.* **2012**, DOI: 10.1002-chem.201200497.
- (28) *Maestro 9.3*, Schrödinger, LLC: New York, 2012.
- (29) Banks, J. L.; Beard, H. S.; Cao, Y.; Cho, A. E.; Damm, W.; Farid, R.; Felts, A. K.; Halgren, T. A.; Mainz, D. T.; Maple, J. R.; Murphy, R.; Philipp, D. M.; Repasky, M. P.; Zhang, L. Y.; Berne, B. J.; Friesner, R. A.; Gallicchio, E.; Levy, R. M. *J. Comput. Chem.* **2005**, *26*, 1752–1780.
- (30) Grimme, S. *J. Comput. Chem.* **2006**, *27*, 1787–1799.
- (31) Cancès, E.; Mennucci, B.; Tomasi, J. J. *Chem. Phys.* **1997**, *107*, 3032–3041.
- (32) Ribeiro, R. F.; Marenich, A. V.; Cramer, C. J.; Truhlar, D. G. *J. Phys. Chem. B* **2011**, *115*, 14556–14562.
- (33) Weigend, F.; Ahlrichs, R. *Phys. Chem. Chem. Phys.* **2005**, *7*, 3297–3305.
- (34) Kruse, H.; Grimme, S. *J. Chem. Phys.* **2012**, *136*, 154101–1–16.
- (35) Goerigk, L.; Grimme, S. *Phys. Chem. Chem. Phys.* **2011**, *13*, 6670–6688.
- (36) Frisch, M. J.; Trucks, G. W.; Schlegel, H. B.; Scuseria, G. E.; Robb, M. A.; Cheeseman, J. R.; Scalmani, G.; Barone, V.; Mennucci, B.; Petersson, G. A.; Nakatsuji, H.; Caricato, M.; Li, X.; Hratchian, H. P.; Izmaylov, A. F.; Bloino, J.; Zheng, G.; Sonnenberg, J. L.; Hada, M.; Ehara, M.; Toyota, K.; Fukuda, R.; Hasegawa, J.; Ishida, M.; Nakajima, T.; Honda, Y.; Kitao, O.; Nakai, H.; Vreven, T.; Montgomery, J. A., Jr.; Peralta, J. E.; Ogliaro, F.; Bearpark, M.; Heyd, J. J.; Brothers, E.; Kudin, K. N.; Staroverov, V. N.; Kobayashi, R.; Normand, J.; Raghavachari, K.; Rendell, A.; Burant, J. C.; Iyengar, S. S.; Tomasi, J.; Cossi, M.; Rega, N.; Millam, J. M.; Klene, M.; Knox, J. E.; Cross, J. B.; Bakken, V.; Adamo, C.; Jaramillo, J.; Gomperts, R.; Stratmann, R. E.; Yazyev, O.; Austin, A. J.; Cammi, R.; Pomelli, C.; Ochterski, J. W.; Martin, R. L.; Morokuma, K.; Zakrzewski, V. G.; Voth, G. A.; Salvador, P.; Dannenberg, J. J.; Dapprich, S.; Daniels, A. D.; Farkas, O.; Foresman, J. B.; Ortiz, J. V.; Cioslowski, J.; Fox, D. J. *Gaussian 09*, revision B.01; Gaussian, Inc.: Wallingford, CT, 2010.
- (37) Rathore, R.; Lindeman, S. V.; Kochi, J. K. *J. Am. Chem. Soc.* **1997**, *119*, 9393–9404.
- (38) Uno, B.; Okumura, N.; Seto, K. *J. Phys. Chem. A* **2000**, *104*, 3064–3072.
- (39) Lotfi, M.; Roberts, R. M. G. *Tetrahedron* **1979**, *35*, 2123–2129.
- (40) Maverick, E.; Trueblood, K. N.; Bekoe, D. A. *Acta Crystallogr., Sect. B* **1978**, *34*, 2777–2781.
- (41) Saheki, M.; Yamada, H.; Yoshioka, H.; Nakatsu, K. *Acta Crystallogr., Sect. B* **1976**, *32*, 662–664.
- (42) Pawlukoć, A.; Sawka-Dobrowolska, W.; Bator, G.; Sobczyk, L.; Grech, E.; Nowicka-Scheibe, J. *Chem. Phys.* **2006**, *327*, 311–318.
- (43) Rosokha, S. V.; Korotchenko, V.; Stern, C. L.; Zaitsev, V.; Ritzert, J. T. *J. Org. Chem.* **2012**, *77*, 5971–5981.
- (44) Zhao, Y.; Truhlar, D. G. *J. Phys. Chem. A* **2004**, *108*, 6908–6918.
- (45) Becke, A. D. *J. Chem. Phys.* **1993**, *98*, 5648–5653.
- (46) Lee, C.; Yang, W.; Parr, R. *Phys. Rev. B* **1988**, *37*, 785–789.
- (47) Guner, V.; Khuong, K. S.; Leach, A. G.; Lee, P. S.; Bartberger, M. D.; Houk, K. N. *J. Phys. Chem. A* **2003**, *107*, 11445–11459.
- (48) Ess, D. H.; Houk, K. N. *J. Phys. Chem. A* **2005**, *109*, 9542–9553.
- (49) Pieniazek, S. N.; Clemente, F. R.; Houk, K. N. *Angew. Chem., Int. Ed.* **2008**, *47*, 7746–7749.